ARMY RESEARCH LABORATORY

Enhanced Target Identification Using Higher Order Shape Statistics

Mark Wellman and Nassy Srour

ARL-TR-1723 February 1999

The findings in this report are not to be construed as an official Department of the Army position unless so designated by other authorized documents.

Citation of manufacturer's or trade names does not constitute an official endorsement or approval of the use thereof.

Destroy this report when it is no longer needed. Do not return it to the originator.

Army Research Laboratory

Adelphi, MD 20783-1197

ARL-TR-1723 **February 1999**

Enhanced Target Identification Using Higher Order Shape Statistics

Mark Wellman and Nassy Srour

Sensors and Electron Devices Directorate

Abstract

The U.S. Army Research Laboratory (ARL) is developing an acoustic target classifier using a backpropagation neural network (BPNN) algorithm. Various techniques for extracting features have been evaluated to improve the confidence level and probability of correct identification (ID). Some techniques used in the past include simple power spectral estimates (PSEs), split-window peak picking, harmonic line association (HLA), principal component analysis (PCA), wavelet packet analysis [1–4], and others. In addition, improved classification results have been obtained when shape statistic features derived from HLA feature sets or seismic PSE features have been incorporated in BPNN training, testing, and cross-validation. The combined acoustic/seismic data from collocated acoustic and seismic sensors are gathered by a three-axis seismic sensor. This is configured as part of an acoustic sensor array that ARL uses on typical field experiments.

The PSE, HLA, and shape statistic feature (SSF) data are extracted from a set of vehicles and then split into a testing and training file. The training file typically consists of 75 percent of the whole data set, and the performance of the trained neural network is evaluated using the remaining test data, and further cross-validation is performed with vehicle data collected at different times of day and various operating conditions. Results of the neural network from a few of the feature extraction algorithms currently under evaluation and from the acoustic/seismic sensor fusion are presented in this report.

Contents

Figures

Tables

1. Introduction

In this report, we discuss the ongoing work at the U.S. Army Research Laboratory (ARL) in feature extraction and classification of ground vehicles based on the fusion of collcated acoustic and seismic sensors. One fundamental problem faced in the classification process is the selection of robust features that are stable and class-specific. Due to several factors, acoustic and seismic signatures are nonstationary in nature [5]. This nonstationary nature greatly enhances the difficulty in the feature selection process, but methods have been reported to somewhat alleviate this difficulty [1,3]. Most notable to date is the use of the harmonic line association (HLA) algorithm with shape statistics [6]. The HLA algorithm takes advantage of spectral characteristics that are dominated by narrow-band spectral peaks. In the past, the narrow-band spectral peaks have been used for classification purposes, either in hierarchical clustering schemes or as direct inputs into an artificial neural network (ANN). The spectral peaks are typically band-limited between 1 and 400 Hz, but peak components occur between 10 and 120 Hz. The majority of tracked and wheeled vehicles of interest are diesel-powered and, thus, the engine firing rate and track slap produce these spectral components. When considering feature methods solely based on the acoustic spectrum, one could often use the entire set of spectral peaks (the power spectral estimate (PSE)) or one can be more clever and select specific frequency components to improve the signal-to-noise ratio (SNR) by using split-window peak picking and/or HLA, which have the added benefit of appreciably reducing the feature space while maintaining class separability.

2. Harmonic Line Association

The HLA technique selects peaks that are harmonically related to create harmonic line sets for each frame (frame = 1 s) of data samples. Split-window peak picking is performed on the PSE feature set first; this takes a fixed window length of 21 bins (~21 Hz bandwidth) and determines the mean energy around the center three or five bins (the split) of the window. If the energy within the split exceeds the mean energy outside, a peak has been detected and will be added to the set of peaks. Using this result, the HLA algorithm finds the maximum peak P in the frequency set and assumes that this peak is some kth harmonic line of the fundamental frequency subject to the following soft constraint for fundamental frequency range,

$$f_{fund} \in \{8,20\} \text{ Hz} \ , \tag{1}$$

and then calculates the total signal strength in this HLA set. The integer value, k, that gives the maximum signal strength is assumed to be the correct harmonic line number, and the harmonic lines of this particular set are retained as a feature vector. This technique has two advantages: (1) the feature vector is normalized and is solely based on the harmonic line number and not a function of frequency and (2) the peak energy is tracked frame to frame, thus producing a predominance pattern for the acoustic energy source [3].

3. Higher Order Shape Statistics

3.1 Background

In the past, the naval community has found shape statistics to be beneficial in certain classification problems. Shape statistic features (SSFs) have been used in evaluating the discrepancy between the correlated and uncorrelated components of return energy in low frequency active target-echo characterization [7]. Also, shape transition statistics have been used in discriminating biologic from manmade sounds by exploiting minute differences in broadband energy [7]. We are not completely unfamiliar with shape statistics since most individuals in science and engineering have had basic probability theory; for example, in defining the characteristics of both discrete and continuous probability distribution functions, one becomes well acquainted with *m*th-order statistics, which are analogous to shape statistics. The defining relationships for shape statistics are the following:

$$\mu_{shape} = \frac{1}{S}\sum_{i=1}^{N} iC(i) \ , \tag{2}$$

$$\theta_{shape} = \sqrt{\frac{1}{S}\sum_{i=1}^{N}\left(i-\mu_{shape}\right)^2 C(i)} \ , \tag{3}$$

$$skewness_{shape} = \frac{1}{S}\sum_{i=1}^{N}\left(\frac{i-\mu_{shape}}{\theta_{shape}}\right)^3 C(i) \ , \tag{4}$$

and

$$kurtosis_{shape} = \frac{1}{S}\sum_{i=1}^{N}\left(\frac{i-\mu_{shape}}{\theta_{shape}}\right)^4 C(i) - 3 \ . \tag{5}$$

Here, S is given by the following:

$$S = \sum_{i=1}^{N} C(i) \ , \tag{6}$$

with $C(i)$ the magnitude for the ith frequency or the harmonic line bin and N the number of bins. In the above, equations (2) and (3) define the shape mean and standard deviation, which are familiar statistical measures. In equation (4), the third-order shape statistic commonly called skewness is defined. Skewness is a measure of the asymmetry around the mean in the distribution and takes on positive or negative values; for example, a distribution with a large tail toward the positive direction would have a positive value for skewness. A Gaussian distribution has zero skewness since such a distribution can be described by the mean and variance

alone. Kurtosis, a fourth-order statistic and defined in equation (5), is a measure of the "peakishness" in a distribution with positive values for a distribution that exhibits strong peaks or is sharper than a normal distribution and negative for flat distributions.

We were motivated to test whether the shape statistics could be used as a means to further reduce the HLA feature space by representing the HLA space with a small set of SSFs. We hope that the multidimension reduction of the HLA space will not drastically reduce separability but will improve BPNN training and reduce complexity. We also would like to investigate the use of these same SSFs as a partially correlated input for the BPNN. We hope that the SSFs may capture characteristics of the HLA distribution in a compact representation that would have a positive influence for the trained BPNN over trained BPNNs that used the HLA features alone. We know that partially correlated features can often enhance classification by neural networks [8].

3.2 Seismic Shape Statistics

The seismic signatures are, to a lesser degree than their acoustic counterparts, wide-band and nonstationary with far fewer narrow-band peaks discernible in their power spectrums. Due to the attenuation of Rayleigh waves, the useful bandwidth for seismic signals is between 10 and 60 Hz [9], with frequencies below 10 Hz being attenuated by the geophone response and frequencies above 60 Hz being mostly ambient and acoustically coupled seismic noise. The use of raw seismic PSEs as a feature vector is much more advantageous than for acoustic features, but we would like to minimize the feature space for practicality. The use of shape statistics for characterizing the energy distribution of seismic spectrums of the different vehicle classes seemed to be prudent. Figures 1 and 2 show the distinctions in power spectrums for tracked versus wheeled seismic signatures.

When one looks carefully at the spectrograms for the seismic data, it is apparent that shape statistics could exploit some of the differences in tracked versus wheeled spectrums and, perhaps, the small changes in the spectral content of various tracked vehicles. Based on these findings, we have investigated the use of the higher order shape statistics and introduced a temporal shape transition statistic for classifying the seismic feature sets. A useful temporal shape transition statistic is simply the absolute change in the shape mean for each subsequent frame. This is given by

$$\Delta mean_{shape}(t) = \mathrm{abs}(\mu_{shape}(t) - \mu_{shape}(t-1)) \,, \tag{7}$$

with an initial value set to zero. The absolute value was selected since it appears to shift the centroid of this feature for tracked versus wheeled targets, thus aiding class separability.

Typically, the predominant seismic energy in our data set falls in the frequency range from 1 to 50 Hz. PSE seismic features simply consist of these 50 frequency bins, and the shape statistics were derived from these

frequency bins as well. Despite the attenuation of the seismic energy below 10 Hz, we believe this region provides useful information for classification purposes. The "raw" seismic PSE features will also be used in the ANN for classification.

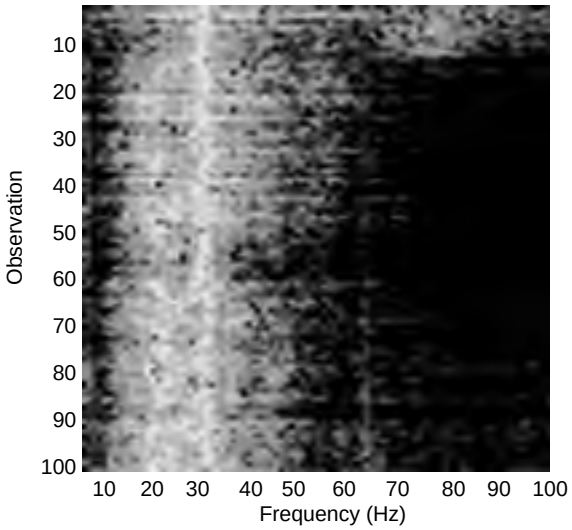

Figure 1. Spectrogram of vertical axis seismic data derived from a tracked vehicle.

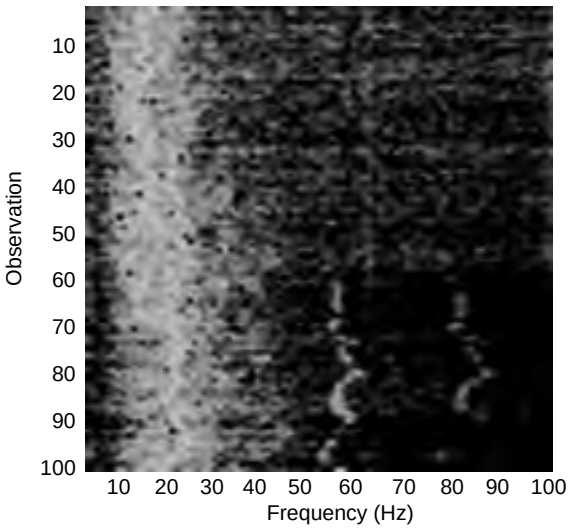

Figure 2. Spectrogram of vertical axis seismic data derived from a wheeled vehicle.

4. Artificial Neural Networks

For target identification (ID), ANNs can provide both a robust classifier and a measure of your confidence in the classification decision. Such networks derive their computational power from the parallel distributed structure and the ability to learn and adapt. Typically, a BPNN is used for the classification procedure. We are currently investigating the performance of other classifier architectures, specifically, "fuzzy" ART maps [8], genetic algorithms [10], and generalized potential neural networks and the application of homogeneous and heterogeneous combinations of classifiers. We will have more to say about their relative merits in future reports. Briefly, these ANNs can give improved classification results in some cases but their complexity is also much greater and becomes an issue in implementation. Through *k*-means analysis, we have seen that HLA data sets exhibit only a few clusters with minor overlap; in this case, a boundary decision classifier like the BPNN should perform well. We employ the BPNN with an adaptive learning rate that allows fine-grain adjustments during training. Smoothing is also incorporated and allows the control of weight adjustment based on the past values of gradient descent and can prevent the training process from terminating in shallow local minimum [8,11]. The general weight update expression when employing smoothing takes the following form:

$$\Delta w(n) = (1-\beta)\eta\delta(n)y(n) + \beta\Delta w(n-1)\,, \tag{8}$$

with β the smoothing constant, η the learning rate, $\delta(n)$ the local gradient, and $y(n)$ the output value for a particular node. (See Haykin [8] for further discussion.)

To qualify the neural network classification performance, a confusion matrix is calculated that provides the percentage of correct identification (C_{ID}) for each class of ground vehicles based on the following expression:

$$C_{ID} = \frac{N_{P_{CID}}}{K}\,, \tag{9}$$

and the confidence levels for classification of each target are calculated by

$$C_{level} = \frac{1}{K}\sum_{i=1}^{K}\left(\sum_{j=1}^{L}\frac{P_{CID_i} - P_{FID_j}}{2(L-1)}\right)\,, \tag{10}$$

with K being the total number of observations and $N_{P_{CID}}$ the number of correct decisions. L in equation 10 is simply the total number of output classes. The value P_{CID_i} is the predicted value of the correct ID for class i, and P_{FID_j} is the predicted value of false ID for class j with respect to class i. P_{CID} is the output for the BPNN output node dedicated to a particular class, and P_{FID} is the output for the other output nodes.

5. Procedure

5.1 Data Collection

Acoustic and seismic data from ground vehicles were gathered at Grayling, Michigan, during the winter with a remote netted acoustic detection system (RNADS) [2,12], which is a remote sensor array architecture. The data set included three tracked and one wheeled vehicle, each powered by a 12-cylinder diesel engine. The remote sensor consists of a triangular array of five microphones with one three-axis geophone (see fig. 3). The seismic sensor provides some unique features that complement the acoustic features. In this report, only the vertical axis seismic data are used for feature extraction.

The acoustic and seismic signals were preamplified with selectable gain of 40 and 60 dB and passed to a ruggedized personal computer (PC) and a digital audio tape recorder (DAT). The acoustic/seismic signatures were then oversampled at a 12-kHz rate by the DAT. Within the PC, acoustic signals are antialiased with a lowpass filter, fed to 16-bit A/D converters, and further processed with a pair of commercially available digital signal processing boards for real-time applications.

5.2 Feature Extraction

Before any feature extraction for classification was performed, the data were filtered and down-sampled to 2 kHz, and high SNR regions of the acoustic and seismic data sets were determined by those regions that gave contiguous harmonic line sets. These are the regions where SNR is high enough that we can detect at least m harmonically related peaks after performing split-window peak picking and thresholding on the acoustic spectrum. The choice of m is somewhat arbitrary but for this experiment $m = 4$; thus, a harmonic line set is considered valid when this condition is met. The observation regions so found were then used specifically for PSE, HLA, HLA shape statistics, and seismic shape statistic processing that would be used in the training, testing, and cross-validation of the BPNN.

PSEs for each 1-s interval of high SNR data were generated using Hanning-windowed short-time Fourier transforms according to the

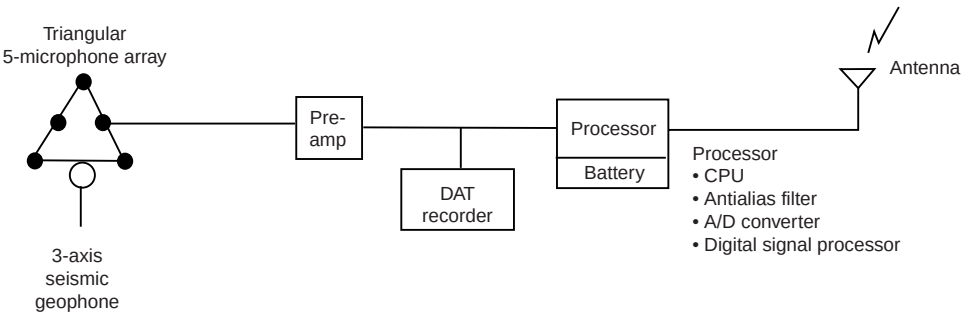

Figure 3. RNADS field sensor and processing architecture.

Welch method [13]. Only the first 200 frequency bins so derived were used for classification purposes.

Seismic time-series data were processed using the same technique to generate the PSEs, and the first 50 frequency bins were used either as inputs to the classifier or were further processed to extract the seismic shape statistics for classification.

6. Results

The following results are the comparisons of the cross-validation using the HLA or the shape statistic space derived from the HLA features. This comparison was made to determine in an ad hoc manner whether the shape statistic features could be beneficial as a multidimension reduction technique, thereby simplifying the classifier design. Within the tables, the value to the far left of the slashes indicates the HLA cross-validation result, and the value to the immediate right is the corresponding result using the shape statistics mean, standard deviation, and skewness alone. Finally, the value to the far right is the cross-validation result using the three shape statistics above with the inclusion of the kurtosis. These results are representative of several trials for each case. The numbers represent the percentage of correct identifications. The BPNN used had an input layer with 3, 4, 11, or 14 input nodes, depending on the feature set, and one hidden layer of 15 nodes and an output layer of 4 nodes.

For these preliminary trials, confidence levels were not calculated. Table 1 shows that the shape statistic features have some discriminatory power but that they are not sufficient when considering their use as a multidimension reduction procedure.

Tables 2 and 3 show the confusion matrix results for a representative trial and they represent the combined cross-validation scores for the HLA features, PSE features, and the addition of the seismic features and seismic shape statistic features using the BPNN. Again, these results are representative of several trials for each case. The numbers represent the percentage of correct identifications. The BPNN used had an input layer from 11 to 250 input nodes, depending on the feature set, and one hidden layer of 15 nodes and an output layer of 3 nodes. Unfortunately, seismic signatures for vehicle class 1 were not available.

Table 2 shows the combined confusion matrices for three target cross-validations using HLA and HLA plus various seismic features. The addition of the seismic skew, kurtosis, and delta mean has increased classification performance. The overall confidence levels for the classification increased from 74 percent for HLA alone to 81 percent for HLA with shape statistics skew, kurtosis, and delta mean. The overall confidence level is simply a weighted average for the individual confidence levels that appear in the table.

Table 1. Harmonic line and shape statistic features.

HLA or HLA shape statistic cross-validations				
	Net output			
Actual	0	1	2	3
0	90/41/15	5/18/35	2/0/0	2/40/48
1	6/9/6	67/65/56	26/0/0	0/25/36
2	0/5/6	6/13/11	93/51/52	0/30/30
3	14/33/11	18/14/14	14/0/7	51/51/66

Table 2. Harmonic line and seismic features.

HLA and HLA with first 50 seismic frequency bins

	Net output			
Actual	0	2	3	Confidence level
0	88/88	0/2	11/8	80/77
2	1/4	80/92	18/3	75/85
3	5/7	2/2	92/89	55/85

HLA and HLA with seismic shape statistics skew and delta mean

	Net output			
Actual	0	2	3	Confidence level
0	88/88	0/3	11/7	80/76
2	1/4	80/90	18/5	75/83
3	5/31	2/0	92/68	55/32

HLA and HLA with seismic shape statistics skew, kurtosis, and delta mean

	Net output			
Actual	0	2	3	Confidence level
0	88/96	0/0	11/4	80/79
2	1/4	80/90	18/6	75/83
3	5/5	2/0	92/95	55/74

The improvement in classification using the addition of the kurtosis in HLA feature space is interesting. Figures 4, 5, and 6 are plots of the seismic shape statistics skew and kurtosis from sample files used in training for the three classes.

One can readily see that the seismic shape statistics for skew and kurtosis are almost linearly separable; thus, a multilayer perceptron like the BPNN classifier performance will improve with their addition [14,15]. These results suggest that one may find it beneficial to develop a hierarchical classifier using these shape statistics in the first stage of classification. A simple linear discriminant classifier should prove to very powerful in this case [14].

Table 3 shows the combined confusion matrices for three-target cross-validation using the PSE and the PSE including the various seismic features.

A few remarks are in order about the training and cross-validation sets used in the experiment. For vehicle class 0 and 1, the training set was fairly comprehensive and the cross-validation was done using a data file from a different time of day and different aspect angle. The vehicle speed and gearing of the data file for cross-validation were represented in the training set. For vehicle class 2, the cross-validation was done with the vehicle from a different time of day and the vehicle was also under load with variable speed and gear, which were partially represented in the training set. The class 3 cross-validation was the severest test, the data file

Table 3. Power spectral estimates and seismic features.

PSE and PSE with first 50 seismic frequency bins

	Net output			
Actual	0	2	3	Confidence level
0	94/100	0/0	5/0	64/83
2	14/0	65/100	20/0	54/80
3	47/47	42/37	10/15	0/0

PSE and PSE with seismic shape statistics skew and delta mean

	Net output			
Actual	0	2	3	Confidence level
0	94/86	0/0	5/13	64/61
2	14/8	65/77	20/14	54/58
3	47/47	42/22	10/30	0/2

PSE and PSE with seismic shape statistics skew, kurtosis, and delta mean

	Net output			
Actual	0	2	3	Confidence level
0	94/86	0/0	5/13	64/67
2	14/8	65/80	20/11	54/61
3	47/50	42/31	10/18	0/0

was from a different time of day, different aspect, and different speed and gear than were represented in the training set. This partly accounts for the poor classification scores in the PSE feature space.

The improvement in the overall confidence levels for classification was greater for the PSE versus PSE plus seismic features as compared with the HLA counterparts, but the maximum overall confidence level for any particular PSE feature space including seismic features was only 70 percent. The maximum individual score increases in confidence for the classification of the classes occurs using the raw seismic features, i.e., the first 50 frequency bins of the seismic PSEs. These improvements are not significantly better than the HLA with seismic shape statistic scores for each class, and considering the reduced complexity of the ANN and the training time and the HLA noise immunity, the HLA with seismic shape statistics feature space appears the more robust.

Figure 4. Skewness versus kurtosis for vehicle class 0 and class 3.

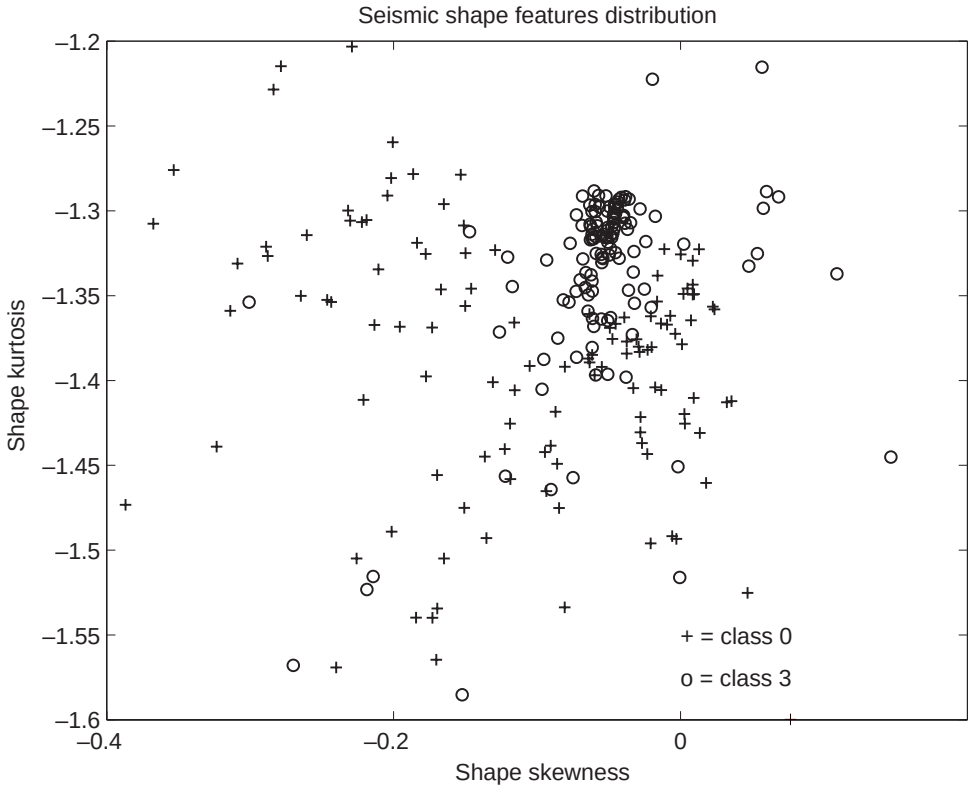

Figure 5. Skewness versus kurtosis for vehicle class 0 and class 2.

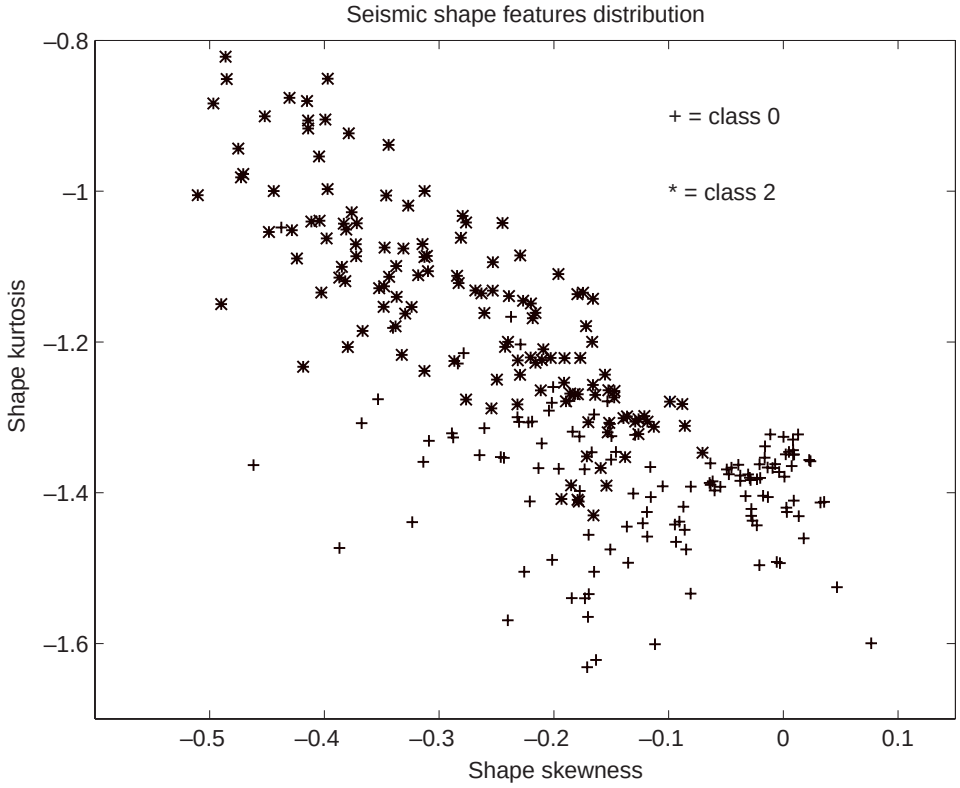

Figure 6. Skewness versus kurtosis for vehicle class 2 and class 3.

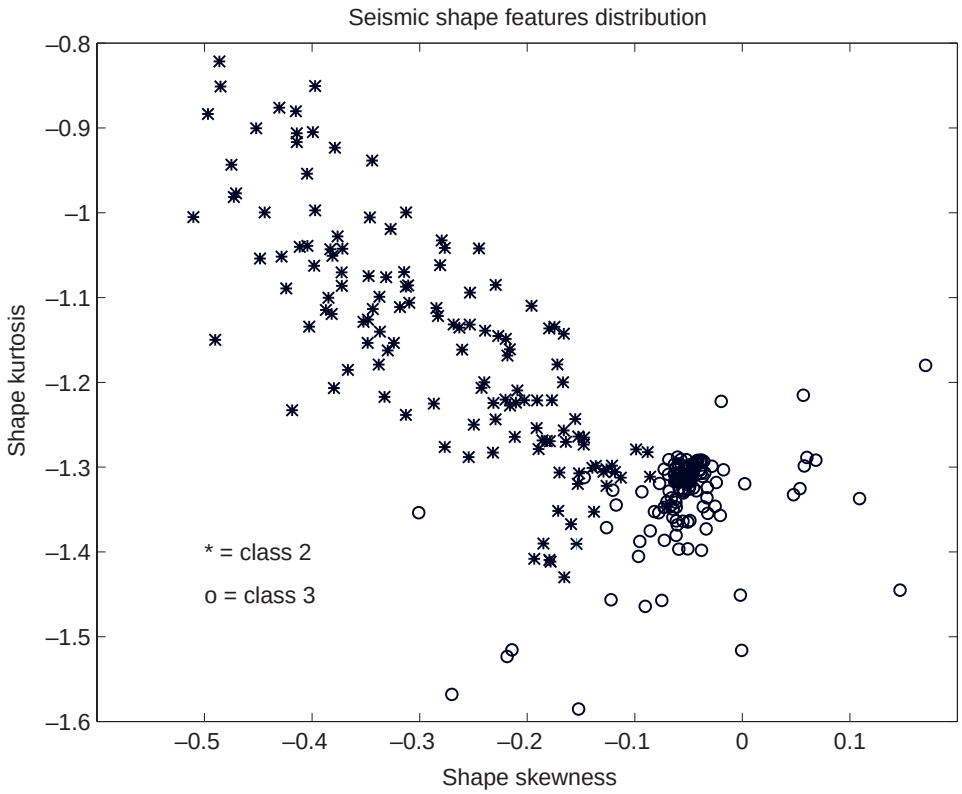

7. Conclusions

The acoustic and seismic detection, tracking, and classification of ground vehicles in a battlefield environment remain challenging problems. The acoustic and seismic signatures of ground vehicles are nonstationary and exhibit both wide-band and narrow-band characteristics. The combined effects of source, terrain, atmospheric propagation, and geologic characteristics can produce large signal variability over the entire range of interest.

We have shown in this preliminary investigation that the inclusion of shape statistics can improve target identification. In addition, the seismic features can act as a powerful discriminant in both the classification of tracked versus wheeled vehicles and increase the separability of tracked vehicles alone. In fact, recent work using only seismic features has produced an average probability of correct ID as high as 86 percent. The seismic shape statistic features look promising in light of the HLA plus seismic shape feature results. The cross-validation scores suggest that this space is far more robust than any features we have investigated to date and it is unlikely that we can improve on the reported scores. These particular three classes of vehicles have presented problems in the past for classification, and we have seen through *k*-means analysis that there can be significant overlap with some feature spaces. Often, class 3 is classified as class 0 and to a lesser extent class 2 when only acoustic features are considered [1,3]. This problem is alleviated with the incorporation of the seismic features.

In future work, we will look at using shape statistics derived from the total spectrum as an additional feature vector combined with the HLA feature space. Experiments will also be performed using only the skewness and kurtosis as additional shape features derived from the original spectrum or HLA feature set. Rank ordering of the shape statistics would be beneficial as well. For the incorporation of seismic signatures, we plan on expanding the number of classes, but further data collection will be needed to validate the HLA plus seismic shape statistic feature space. Obviously, there are a great number of variables to consider in the data collection/validation process to further test classifier robustness. We also plan to address the sensitivity of the shape statistics to outliers in the classification process. Skewness and kurtosis can be quite sensitive to outliers and, therefore, give erroneous results in these cases.

Acknowledgments

This work was performed in-house by the Sensors and Electron Devices Directorate's Acoustic Signal Processing Branch at ARL in Adelphi, Maryland. The authors would like to acknowledge the beneficial discussions with Rama Chellappa of the University of Maryland, Kie Eom of the George Washington University, and David Hillis of the Intelligent Systems Branch at ARL.

References

1. M. Wellman, N. Srour, and D. Hills, *Acoustic Feature Extraction for a Neural Network Classifier*, U.S. Army Research Laboratory, ARL-TR-116 (January 1997).

2. N. Srour and J. Robertson, *Remote Netted Acoustic Detection System: Final Report*, Army Research Laboratory, ARL-TR-706 (April 1995).

3. J. A. Robertson and B. Weber, *Artificial Neural Networks for Acoustic Target Recognition*," joint report by ARL and ITT Research (1993).

4. K. Eom, R. Chellappa, M. Wellman, N. Srour, and D. Hillis, "Acoustic Target Classification Using Multiscale Methods," *U.S. ARL 1997 Sensors and Electron Devices Symposium Proceedings* (January 1997).

5. N. Berg, N. Srour, and G. Prado, *Unattended Ground Sensor Performance, Prediction and Preliminary System Requirements* (1993).

6. M. Wellman and N. Srour, "Feature Extraction for a Neural Network Classifier," *3rd Joint Meeting of Acoustical Society of America and Acoustical Society of Japan* (December 1996).

7. F. B. Shin and D. H. Kil, *Pattern Recognition and Prediction with Applications to Signal Characterization*, American Institute of Physics, Woodbury, NY (1996).

8. S. Haykin, *Neural Networks, A Comprehensive Foundation*, Macmillan Publishing Company, NJ (1994).

9. G. Prado and P. Martel, *Design and Test of a Seismic Capability for the RNADS Sensor*, SenTech, Inc., report for U.S. Army Research Laboratory, Adelphi, MD (February 1994).

10. D. Goldberg, *Genetic Algorithms in Search, Optimization, and Machine Learning*, Addison-Wesley, Reading, MA (1989).

11. *Database Mining Workstation*, Reference Manual, HNC, Inc. (1992).

12. S. Choy, M. Fong, and H. Vu, *Software Architecture for an Expandable Testbed Sensor Tracking System*, internal ARL technical report (1995).

13. P. D. Welch, "The Use of Fast Fourier Transforms for Estimation of Power Spectra," *IEEE Trans. Audio-Electroacoustics*, **15** (June 1970), pp 70–73.

14. K. Fukunaga, *Introduction to Statistical Pattern Recognition, 2nd edition*, Academic Press, San Diego (1990).

15. R. O. Duda and P. E. Hart, *Pattern Classification and Scene Analysis*, John Wiley and Sons, Inc. (1973).

Distribution

Admnstr
Defns Techl Info Ctr
Attn DTIC-OCP
8725 John J Kingman Rd Ste 0944
FT Belvoir VA 22060-6218

DIA Central Masint Ofc
Attn P Demos
Attn CPT M Donofrio
3100 Clarendon Blvd
Arlington VA 22201

Ofc of the Dir Rsrch and Engrg
Attn R Menz
Pentagon Rm 3E1089
Washington DC 20301-3080

Ofc of the Secy of Defns
Attn ODDRE (R&AT)
Attn ODDRE (R&AT) S Gontarek
The Pentagon
Washington DC 20301-3080

OSD
Attn DUSD/AT C Perkins
Pentagon Rm 3E1065
Washington DC 20301-2500

OSD
Attn OUSD(A&T)/ODDR&E(R) R J Trew
The Pentagon
Washington DC 20301-7100

AATD (ATCOM)
Attn AMSAT-R-TU L Sutton
FT Eustis VA 22604

AMCOM MRDEC
Attn AMSMI-RD W C McCorkle
Redstone Arsenal AL 35898-5240

ARL/SLAD
Attn AMSRL-SL-EV O A Payan
White Sands Missile Range NM 88002-5513

Army Spc and Strtgc Defns
Attn CSSD-TC-C R N Adams
PO Box 1500
Huntsville AL 35807-3801

CECOM
Attn PM GPS COL S Young
FT Monmouth NJ 07703

Dept of the Army DCS for Intllgnc
Attn DAMI-POB B Allen
Washington DC 20301-1001

Dir for MANPRINT
Ofc of the Deputy Chief of Staff for Prsnnl
Attn J Hiller
The Pentagon Rm 2C733
Washington DC 20301-0300

Hdqtrs Dept of the Army
Attn DAMO-FDT D Schmidt
400 Army Pentagon Rm 3C514
Washington DC 20301-0460

INSCOM
Dept of the Army
Attn B Kitchen
Attn E Bielecki
Attn M Woodford
8825 Beulah Stret
FT Belvoir VA 22060-5246

NVESD
Attn AMSEL-RD-NV-GSID T Smith
Attn AMSEL-RD-NV-TIS J A Rarick
Attn AMSEL-RD-NV-SS-GV J Brooks
Attn AMSEL-RD-NV-TIS T Anderson
Attn AMSRL-RD-NV-UAB C Walters
Attn AMSEL-RD-NV-VISP-CR G Klager
Attn AMSEL-RD-NV-SS-TPS P Lundy
Attn AMSEL-RD-NV-TIS-PS D Rehek
Attn AMSRL-RD-NV-SS-GV R Volpone
10221 Burbeck Rd
FT Belvoir VA 22060

TASC
Attn D S Bishop
1992 Lewis T Gurner
FT Walton FL 32547-1255

Distribution (cont'd)

US Army AFDD
Attn AMSAT-R-AF D Boxwell
Attn M/S 219-3 W Mosher
Ames Rsrch MS N215-1
Moffett Field CA 94035

US Army ARDEC
Attn AMSTA-AR-FSF-RM J Heberley
Bldg 95N
Picatinny Arsenal NJ 07806

US Army Armament Rsrch Dev & Engrg Ctr
Attn AMSTA-AR-TD M Fisette
Bldg 1
Picatinny Arsenal NJ 07806-5000

US Army ATCOM
Attn AMSAT-R-TV M Dinning
Attn AMSAT-R-TV G Birocco
FT Eustis VA 23604-5577

US Army CECOM
Attn AMSEL-RD-NV-CI-NCTR L Stein
FT Monmouth nJ 07703-5206

US Army CECOM/NVESD
Attn AMSEL-RD-NV-RD-IFF M Muller
FT Monmouth NJ 07703

US Army CRREL
Attn CECL-GP M Moran
72 Lyme Rd
Hanover NH 03755-1290

US Army Edgewood RDEC
Attn SCBRD-TD G Resnick
Aberdeen Proving Ground MD 21010-5423

US Army Info Sys Engrg Cmnd
Attn ASQB-OTD F Jenia
FT Huachuca AZ 85613-5300

US Army MICOM
Attn AMSMI-RD-MG-IP M W Harper
Bldg 5400
Redstone Arsenal AL 35898

US Army Natick
Attn SSCNY-YB J B Sampson
Natick MA 01760-5020

US Army Natick RDEC
Acting Techl Dir
Attn SSCNC-T P Brandler
Natick MA 01760-5002

Director
US Army Rsrch Ofc
4300 S Miami Blvd
Research Triangle Park NC 27709

US Army Rsrch Ofc
Attn AMXRO-PH J Lavery
Attn AMXRO-PH M Ciftan
PO Box 12211
Research Triangle Park NC 27709-2211

US Army Simulation, Train, & Instrmntn Cmnd
Attn J Stahl
12350 Research Parkway
Orlando FL 32826-3726

US Army TACOM
Attn AMSTA-TR-S E Shalis
Warren MI 48090

US Army Tank-Automtv Cmnd Rsrch, Dev, & Engrg Ctr
Attn AMSTA-TA J Chapin
Warren MI 48397-5000

US Army Train & Doctrine Cmnd
Battle Lab Integration & Techl Dirctrt
Attn ATCD-B J A Klevecz
FT Monroe VA 23651-5850

US Military Academy
Mathematical Sci Ctr of Excellence
Attn MDN-A MAJ M D Phillips
Dept of Mathematical Sci Thayer Hall
West Point NY 10996-1786

USA ATC
Attn STECS-AC-TE-A G Rogers
Aberdeen Proving Ground MD 21005-5059

Distribution (cont'd)

USA NGIC
Attn IANG-RSG B Grachus
Attn SRA-ELLIOTT C Elliott
220 7th Stret NE
Charlottesville VA 22902

USAE Waterways Experimental Sta
Attn CEWES-SD-R B L Carnes
3909 Halls Ferry Rd
Vicksburg MS 39180-6199

Nav Surface Warfare Ctr
Attn Code B07 J Pennella
17320 Dahlgren Rd Bldg 1470 Rm 1101
Dahlgren VA 22448-5100

US Nav Postgraduate Schl
Dept of Physics
Attn K Woehler
Monterey CA 93943

Chicken Little Joint Proj
Attn 46 OG/OGML J A Sledge
104 Cherokee Ave
Eglin AFB FL 32542-5600

Lawrence Livermore Natl Lab
Attn M/S L-183 J Baker
7000 East Ave
Livermore CA 94550

DARPA
Attn ASTO T Kooij
Attn B Kaspar
Attn E Carapezza
Attn R Dugan
3701 N Fairfax Dr
Arlington VA 22203-1714

NASA Langley Rsrch Ctr
Aeroacoustics Branch
Attn A W Mueller
Fluid Mechanics MS-461
Hampton VA 23681

Johns Hopkins Univ
Applied Physics Lab
Attn A Coon
Johns Hopkins Rd
Laurel MD 20723-6099

Penn State Univ
Appd Rsrch Lab
Attn K C Reichard
Attn D C Swanson
PO Box 30
State College PA 16804

Penn State Univ
Dept of Geosciences
Attn R J Greenfield
Deike Bldg
University Park PA 16801

Univ of Maryland
Dept of Elec Engrg
Attn K-B EOM
Attn R Chellappa
Rm 2365 A V Williams Bldg
College Park MD 20742-3285

Univ of Maryland
Elect Engrg Dept
Attn S Shamma
Attn R Liu
College Park MD 20742-3275

Univ of Michigan
EECS Dept
Attn W J Williams
Systems Div
Ann Arbor MI 48109-2122

Univ of Mississippi
NCPA
Attn H E Bass
University MS 38577

Univ of Texas
Appld Rsrch Lab
Attn M B Bennett
Attn N Bedford
PO Box 8029
Austin TX 78713-8029

BBN Sys & Technologies
Attn T Galaitsis
70 Fawcett Stret
Cambridge MA 02138

Distribution (cont'd)

Draper Lab
Image Recognition Sys
Attn M Desai
Attn MS 37 J Bernstein
Attn MS 37 P Rosenstrach
555 Technology Sq
Cambridge MA 02139

ENSCO Advncd Tech & Planning
Attn T Cirillo
Attn T Gamble
5400 Port Royal Rd
Springfield VA 22151

Hicks & Associates, Inc
Attn G Singley III
1710 Goodrich Dr Ste 1300
McLean VA 22102

Hughes Ground Sys Grp
Attn K Kohnen
PO Box 3310 MS E242
Fullerton CA 92634-3310

Hughes Undersea Sys Div
Attn M Rakijas
PO Box 3310 MS 604/E242
Fullerton CA 92834-3310

Lockheed Martin Comm Sys
Attn P Walter
Attn S Mui
1 Federal Stret
Camden NJ 08102

Lockheed Sanders Inc
Attn S W Lang
PO Box 2057
Nashua NH 03061-0868

Lockheed-Sanders
Attn PTP02-A001 D Deadrick
PO Box 868
Naushua NH 03061-0868

MIT Lincoln Lab
Attn S4-307B R Lacoss
244 Wood Stret
Lexington MA 02173-9108

Mitre Corporation
Attn C Burmaster
1820 Dolley Madison
McLean VA 22102-3481

Northrop Corp
Attn W350/N6 Y-M Chen
PO Box 5032
Hawthrone CA 90251-5032

Palisades Inst for Rsrch Svc Inc
Attn E Carr
1745 Jefferson Davis Hwy Ste 500
Arlington VA 22202-3402

Textron Defns Sys
Program Dev Tactical Sys
Attn R J Correia
Attn R L Steadman
201 Lowell Stret
Wilmington MA 01887

US Army Rsrch Lab
Attn AMSRL-SL-EV K Morrison
White Sands Missile Range NM 88002-5513

US Army Rsrch Lab/HRED
Attn AMSRL-HR-SD J Kalb Bldg 520 Rm 28
Attn AMSRL-HR-SD T Letowski
Bldg 520 Rm 39
Aberdeen Proving MD 21005

US Army Rsrch Lab
Attn AMSRL-D R W Whalin
Attn AMSRL-DD J Rocchio
Attn AMSRL-CI-LL Techl Lib (3 copies)
Attn AMSRL-CS-AS Mail & Records Mgmt
Attn AMSRL-CS-EA-TP Techl Pub (3 copies)
Attn AMSRL-IS J D Gantt
Attn AMSRL-IS-C LTC M R Kindl
Attn AMSRL-IS-CI B Broome
Attn AMSRL-IS-CI D Hillis
Attn AMSRL-IS-CI T Mills
Attn AMSRL-SE-RU H Khatri
Attn AMSRL-SE-SA J Eicke
Attn AMSRL-SE-SA M Wellman (5 copies)
Attn AMSRL-SE-SA N Srour
Adelphi MD 20783-1197

REPORT DOCUMENTATION PAGE

Form Approved
OMB No. 0704-0188

1. AGENCY USE ONLY *(Leave blank)*	2. REPORT DATE	3. REPORT TYPE AND DATES COVERED
	January 1999	Interim, January to May 1997

4. TITLE AND SUBTITLE Enhanced Target Identification Using Higher Order Shape Statistics

5. FUNDING NUMBERS

DA PR: AH16
PE: 62120A

6. AUTHOR(S) Mark Wellman and Nassy Srour

7. PERFORMING ORGANIZATION NAME(S) AND ADDRESS(ES)
U.S. Army Research Laboratory
Attn: AMSRL-SE-SA email: mwellman@arl.mil
2800 Powder Mill Road
Adelphi, MD 20783-1197

8. PERFORMING ORGANIZATION REPORT NUMBER
ARL-TR-1723

9. SPONSORING/MONITORING AGENCY NAME(S) AND ADDRESS(ES)
U.S. Army Research Laboratory
2800 Powder Mill Road
Adelphi, MD 20783-1197

10. SPONSORING/MONITORING AGENCY REPORT NUMBER

11. SUPPLEMENTARY NOTES
ARL PR: 8NE4TI
AMS code: 622120.H16

12a. DISTRIBUTION/AVAILABILITY STATEMENT Approved for public release; distribution unlimited.

12b. DISTRIBUTION CODE

13. ABSTRACT *(Maximum 200 words)*

The U.S. Army Research Laboratory (ARL) is developing an acoustic target classifier using a backpropagation neural network (BPNN) algorithm. Various techniques for extracting features have been evaluated to improve the confidence level and probability of correct identification (ID). Some techniques used in the past include simple power spectral estimates (PSEs), split-window peak picking, harmonic line association (HLA), principal component analysis (PCA), wavelet packet analysis [1–4], and others. In addition, improved classification results have been obtained when shape statistic features derived from HLA feature sets or seismic PSE features have been incorporated in BPNN training, testing, and cross-validation. The combined acoustic/seismic data from collocated acoustic and seismic sensors are gathered by a three-axis seismic sensor. This is configured as part of an acoustic sensor array that ARL uses on typical field experiments.

The PSE, HLA, and shape statistic feature (SSF) data are extracted from a set of vehicles and then split into a testing and training file. The training file typically consists of 75 percent of the whole data set, and the performance of the trained neural network is evaluated using the remaining test data, and further cross-validation is performed with vehicle data collected at different times of day and various operating conditions. Results of the neural network from a few of the feature extraction algorithms currently under evaluation and from the acoustic/seismic sensor fusion are presented in this report.

14. SUBJECT TERMS	15. NUMBER OF PAGES
Target identification, shape statistics, feature fusion	27
	16. PRICE CODE

17. SECURITY CLASSIFICATION OF REPORT	18. SECURITY CLASSIFICATION OF THIS PAGE	19. SECURITY CLASSIFICATION OF ABSTRACT	20. LIMITATION OF ABSTRACT
Unclassified	Unclassified	Unclassified	UL

NSN 7540-01-280-5500

Standard Form 298 (Rev. 2-89)
Prescribed by ANSI Std. Z39-18
298-102

DEPARTMENT OF THE ARMY
U.S. Army Research Laboratory
2800 Powder Mill Road
Adelphi, MD 20783-1197